



The effect of solvent size on physical gelation in triblock copolymer solutions

Yunqi Li, Zhaoyan Sun, Zhaohui Su, Tongfei Shi, and Lijia An

Citation: *J. Chem. Phys.* **122**, 194909 (2005); doi: 10.1063/1.1900043

View online: <http://dx.doi.org/10.1063/1.1900043>

View Table of Contents: <http://jcp.aip.org/resource/1/JCPSA6/v122/i19>

Published by the [American Institute of Physics](#).

Additional information on J. Chem. Phys.

Journal Homepage: <http://jcp.aip.org/>

Journal Information: http://jcp.aip.org/about/about_the_journal

Top downloads: http://jcp.aip.org/features/most_downloaded

Information for Authors: <http://jcp.aip.org/authors>

ADVERTISEMENT

**ACCELERATE AMBER AND NAMD BY 5X.
TRY IT ON A FREE, REMOTELY-HOSTED CLUSTER.**

[LEARN MORE](#)

The effect of solvent size on physical gelation in triblock copolymer solutions

Yunqi Li, Zhaoyan Sun, Zhaohui Su, Tongfei Shi,^{a),b)} and Lijia An^{a),c)}

State Key Laboratory of Polymer Physics and Chemistry, Changchun Institute of Applied Chemistry, Chinese Academy of Sciences, Graduate School of the Chinese Academy of Sciences, 5625 Renmin Street, Changchun 130022, People's Republic of China

(Received 8 February 2005; accepted 9 March 2005; published online 17 May 2005)

The gelation of physically associating triblock copolymers in a good solvent was investigated by Monte Carlo simulation, and the effect of the solvent size on the gelation was discussed in detail. The solvent size can greatly affect the conformation distribution of the polymer chains, the size distribution of the micelle, and the mechanism of the gelation on microscale, mesoscale, and macroscale. Our results indicate that the effect of the solvent size on the physical gelation exhibits three distinct regions. The gelation closely couples to the chain conformation transition when the solvent size is normal or quasinormal; the gelation occurs simultaneously with phase separation when the solvent size approaches the ideal end-to-end distance of the polymer chains; the gelation follows a glass transition mechanism upon increasing the solvent size to much larger than the ideal end-to-end distance of polymer chains. We also found that the volume fraction of the gel point can shift from 0.20 to 0.06, a range much broader than that reported in the literature. © 2005 American Institute of Physics. [DOI: 10.1063/1.1900043]

INTRODUCTION

Polymeric gels played an important role as soft matter resources in many fields such as biology,^{1–4} material engineering,⁵ and pattern design.⁶ These gels can exhibit very interesting physical properties, one of which is the sol-gel transition process. The sol-gel transition method turns out to be a powerful tool for synthesizing new functional materials or purifying materials under control.⁷ Therefore, physical gelation in polymer solutions remains a subject of intense study.

In the past two decades, many researches have been carried out to explore the nature of the physical gelation process in polymer solutions. It was found that physical gelation is sensitive to many factors,^{8,9} such as temperature, concentration^{10–13} and composition of the polymer,¹⁴ and ionic strength.¹⁵ Many mechanisms have been proposed to describe the physical gelation, the majority of them treating gelation as percolation.¹⁶ In summary, most of these mechanisms can be categorized into three classes: (1) the gelation is considered as a subglass transition, and the formation of gel network is due to the crowd of the gel components and the arrest of these components by the cage arouse from the attractive or the repulsive potential among the components.^{17–22} A representative case well described by this type of mechanisms is a mixture of polymer, colloid or protein, and solvent. (2) The gelation takes place with the concomitance of phase separation, and the gelation is a process where polymer chains randomly aggregate.^{23–27} This type of mechanisms has successfully applied in treating polymer so-

lutions with selective solvent. (3) The gelation closely couples to chain conformation transition, and the gelation is determined by the extent of bridging of micelle or the number of chains with bridge conformation.^{28–33} Typical systems are well described by these mechanisms including self-assembly polymer solutions. However, each of these mechanisms is only valid for some systems. There is not any universal mechanism that can satisfactorily describe all the physical gelation processes.

On the other hand, we have noticed that changing the size of solvent molecules can affect the phase behavior of polymer solutions. It has been found that mixtures containing polymers, colloids or proteins, and a solvent have displayed many interesting self-assembly structures and abundant phase diagrams,^{34–36} such as the reentrance to glassy state phenomenon and the jamming phenomenon, etc. These literature reports on the change in the properties of polymer solutions have inspired the research on the effect of the solvent size on polymer solution properties.³⁷ For example, in order to present a concise description for their experimental results, Zhou *et al.*^{38,39} proposed the term *middle-sized solvent* and concluded that addition of this kind of solvent has significant effect on the properties of a polymer solution. They found that adding a middle-sized polyethyl glycol oligomer (PEG) into a concentrated solution of *i*PS or *i*PMMA can enhance the crystallization kinetics of the polymer from the solution and lead to a higher crystallinity, which may be due to less entanglements among polymer chains caused by the middle-sized solvent.

In theoretical treatment or experimental research, most of the mechanisms proposed to date for physical gelation in polymer solutions are based on solvent of normal size. However, the solvent size plays an important role in the phase

^{a)}Authors to whom correspondence should be addressed.

^{b)}Fax: +86-431-5262126. Electronic mail: tfshi@ciac.jl.cn

^{c)}Fax: +86-431-5685653. Electronic mail: ljan@ciac.jl.cn

behavior of polymer solutions, including the physical gelation. Even though there have been many reports either on physical gelation in polymer solutions or on the effect of solvent size on the phase behavior of polymer solutions, research combining both aspects together is still absent. Whether the dependence of polymer solution properties to the changing of the solvent size is monotonic or not is still unknown. A clear understanding of the relationship between them may afford an effective handle to control gelation processes if the solvent size can strongly affect the gelation. The investigation of the effect of solvent size on the physical gelation would aid further understanding of the physical gelation process.

In this work, we study the effect of solvent size on the physical gelation in solutions of a triblock copolymer solution under good solvent condition. In this paper, we first present the model and the methods used in the study and then report the effect of solvent size on the phase diagram of sol-gel coexistence, the aggregation behavior, and the conformation distribution of the polymer chains, and finally we discuss different mechanisms of gelation in different regions of solvent size.

SIMULATION MODEL

The simulation was carried out in a coarse-grained lattice in consideration of the computational tractability and the important qualitative features of real polymers.³⁹ Each monomer occupied a whole unit cell of eight sites in a three-dimensional periodic simple cubic lattice. Neighboring monomers along the same polymer chain were connected via one of the 108 possible bond vectors. Thermal interactions were catered for by a short cutoff range which was set at $\sqrt{6}$ in this work, ensuring that the first peak of the correlation function is encompassed by the range of the potential.⁴⁰ The system was equilibrated through a combination motion of bond-fluctuation model^{41,42} (BFM) and snake creep.⁴³ The elemental attempt motions of the bond fluctuation and the snake creep were (100) and the snake-creep attempts only occurred when the random attempting motion was on the head or the tail monomer of the polymer chain. The attempted relaxation motions were realized by the random diffusion of voids⁴⁴ and governed by the Metropolis sampling rule.⁴⁵

The architecture of the triblock copolymer is set as $A_{15}B_{20}A_{15}$, where the subscripts represent the number of monomers in each block. The number of polymer chains n_p is set to $V\phi/8l_p$, where $V \equiv 128^3$ is the total number of sites in the cubic lattice with periodic boundary conditions in all directions, the coefficient 8 coming from the model where 8 lattice sites were occupied by each monomer, ϕ is the volume fraction of the polymer, and l_p is the number of monomers in each polymer chain. The number of the linear solvent molecules n_s is set to $(0.95 - \phi)V/8l_s$, where l_s is the number of monomers in each solvent molecule. In addition to the polymer and the solvent, the rest are filled with voids. Nearest neighboring pairs of monomers have interaction energies as follows: $\varepsilon_{AA} = -0.5k_B T$, $\varepsilon_{AS} = \varepsilon_{BS} = -0.1k_B T$, where

the subscriptions A , B , and S represent the monomers in block A , block B , and solvent molecules, respectively, and all other interaction energies are null.

To generalize the scenario concerning the effect of the solvent size, we use the dimensionless parameter $\xi = l_p^{1/2}/l_s$ proposed by de Gennes⁴⁶ as the size ratio to label the solvent size, where l_p is set at 50 and l_s varies from 1 to 20. The gel formation in this system is through the attractive potential among the monomers in A blocks. The gelation is treated as percolation based on the percolation theory introduced by Stauffer and Aharony.⁴⁷ The phase diagram of the sol-gel coexistence is determined through the sigmoidal-Boltzmann equation fit to the simulative result of the percolation probability³³ $P(\xi, \phi)$ which is written as

$$P(\xi, \phi) = N_p(\xi, \phi)/N_t, \quad (1)$$

where $N_p(\xi, \phi)$ is the number of percolated samples at each ξ and ϕ , and N_t is the number of parallel samples, which is set at 25. The 25 parallel samples at each size ratio and volume fraction in this work were also used to obtain more accurate results. They were generated as follows: the polymer chains, the solvent molecules, and the voids were evenly placed in the cubic lattice at first, and then the configuration was relaxed without any interactions for 1×10^5 Monte Carlo steps (MCS), each MCS representing the time that every monomer in the polymer chain had one attempt to move in average, a relaxation time long enough to eliminate any artificial factors, and finally these parallel samples were generated with all the interaction energies "switch on" for 5×10^5 MCS trails on different random sequences.

RESULTS AND DISCUSSION

The relationship of the percolation probability $P(\xi, \phi)$ with the volume fraction and the size ratio is first investigated in order to determine the critical points of the gelation using the theoretical approach described in our previous publication.³³ Figure 1(a) shows that the sigmoidal-Boltzmann equation fits the simulation data well, which suggests that the theoretical approach is valid for treating this system. There are two critical points in the volume fraction correlating to the sol-gel transition at each fixed size ratio, the lower (ϕ_c) and the upper ($\phi_{U,c}$) critical volume fractions, and the lower critical point is also called the gel point. When the volume fraction is lower than ϕ_c , gel cannot form in any sample; when $\phi_c < \phi < \phi_{U,c}$, gel forms in some of the samples; when the volume fraction is higher than $\phi_{U,c}$ gel always exists in every sample. Figure 1(b) shows the effect of solvent size on the phase diagram of the sol-gel coexistence. It can be seen that the critical volume fraction varies nonmonotonically with decreasing of the size ratio (i.e., increasing of the solvent size). For the convenience of discussion, we divide the size ratio range into three regions: in region I, $\xi \ll 1$; in region II, $\xi \approx 1$, and in region III, $\xi > 1$. From Fig. 1(b), it can be seen that in region III, with the size ratio decreasing, the two critical volume fractions of the gelation first gradually shift to lower polymer concentrations with a small fluctuation before they approach region II, and each reaches a minimum in region II, and then they sharply

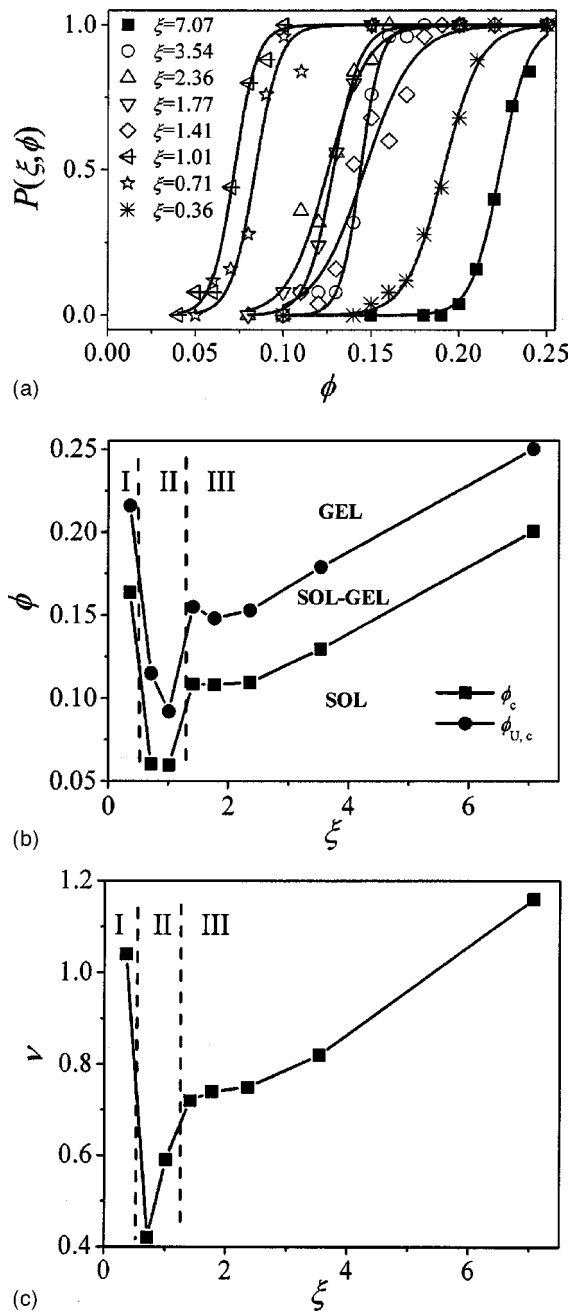


FIG. 1. (a) The relationship of the percolation probability with the volume fraction and the size ratio; the solid lines are the sigmoidal-Boltzmann equations fit to the simulation data; (b) the dependence of the critical volume fraction of the gelation on the size ratio. The vertical dash lines are the boundaries between different size regions; (c) the scaling exponents as a function of the size ratio.

shift back to higher polymer concentrations in region I. In their investigation on the critical volume fraction ϕ_c , Nguyen-Misra and Matice⁴⁸ have found that the critical volume fraction ϕ_c can shift from 0.10 to 0.06 for ABA triblock copolymers in selective solvents. However, ϕ_c in our system can change from 0.20 ($\xi=7.07$) to 0.06 ($\xi=1.01$), a volume fraction range much broader than any previously reported values. On the other hand, Bohbot-Raviv *et al.*⁴⁹ have observed that addition of single-ended polymers can dissolve an existed gel network. This similar dissolution of gel also can be realized in our system by changing the solvent size at

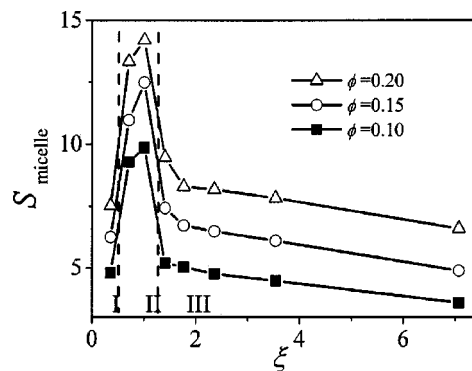


FIG. 2. The dependence of the average micelle size on the size ratio. The vertical dash lines have the same meaning as that in Fig. 1(b).

a fixed volume fraction larger than 0.06. In addition, we observed that the solvent size can greatly affect the scaling behavior of $P(\xi, \phi) \propto (\phi - \phi_c)^\nu$, too. The scaling exponent ν as a function of the size ratio is plotted in Fig. 1(c). It follows a similar trend as the critical volume fraction of the gelation. In our previous work,³³ we found that the decrease of the exponent corresponds to a stronger attractive potential among the monomers in the A blocks. Compared with the ν 's in other regions, the ν 's in region II are very small, which implies that the solvent has induced an extra attractive potential among the polymer chains.

The above results illustrate that the effect of solvent size on gelation is nonmonotonic and rather complicated. In order to explore the reason, the size distribution of the micelle at mesoscale and the conformation distribution of the polymer chains at microscale are investigated, respectively. The size distribution of the micelle is defined as

$$f_i = \langle n_m \rangle n_i / 2n_p, \quad (2)$$

where n_i is the number of the A blocks in the i th micelle, $n_i=0, 1, \dots, 2n_p$, n_m is the number of the micelle containing n_i A blocks, and the $\langle \rangle$ denotes the ensemble average of the 25 parallel samples at each size ratio and volume fraction. Then the average micelle size in unit of A block can be obtained from

$$\bar{S} = 2n_p / \langle \sum n_m \rangle, \quad (3)$$

where the coefficient 2 is from the fact that there are two A blocks in each copolymer chain, and the $\langle \rangle$ has the same meaning as in Eq. (2). Figure 2 shows that in the sol-gel transition regime, with decreasing of the size ratio for a given volume fraction, the average micelle size increases in region III, reaches a maximum in region II, and then it decreases sharply in region I. It is obvious that in region II the solvent can lead to extra aggregation of the micelle, which may have contributed to the appearance of the minimum of the volume fraction of the gel point. The dependence of the size distribution of the micelle on the volume fraction at different size ratio regions is shown in Fig. 3. It can be seen that when the volume fraction increases, in region I, the micelle size distribution becomes narrower [Fig. 3(a)], while in region II, the distribution broadens significantly [Fig. 3(b)]. In region III, with increasing volume fraction at lower ξ , the

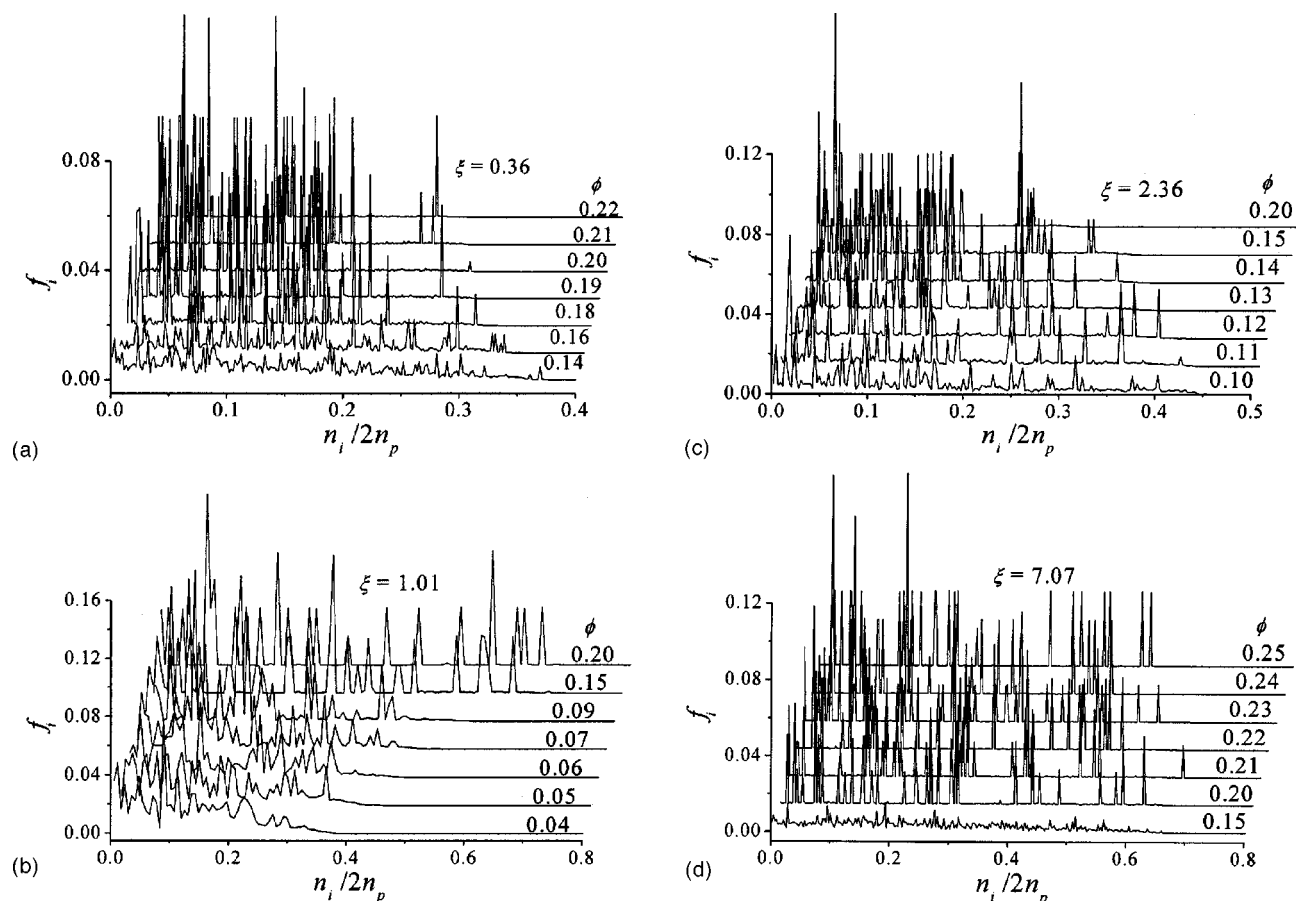


FIG. 3. Typical micelle size distribution changing with the volume fraction in different regions of the size ratio: (a) region I; (b) region II; (c) and (d) region III.

size distribution narrows down slightly [Fig. 3(c)] and no clear trend is found at high ξ [Fig. 3(d)]. These results show that at mesoscale the solvent size has clear effect on the micelle aggregation behavior.

There are four types of chain conformation in this system, dangling, free, loop, and bridge conformations, which have been defined in our previous report,³³ and the effect of solvent size on the conformation distribution in the sol-gel transition regime is shown in Fig. 4. Since the dangling chains and the free chains only account for a small fraction of the chains in the sol-gel transition regime, their contribution to the gelation can be neglected, therefore, we only consider the distribution of the chains in loop conformation and bridge conformation. It is found that the fraction of the loop chains (f_{loop}) increases quickly with ξ in region I and reaches a maximum in region II. In region III, f_{loop} does not change much with ξ [Fig. 4(a)]. The shape of the plot is very similar to that for the dependence of the average micelle size on ξ . The dependence of the fraction of the bridge chains (f_{bridge}) on the size ratio is plotted in Fig. 4(b), showing almost the opposite trend as that of Fig. 4(a), which is understandable, because $f_{\text{loop}} + f_{\text{bridge}} \approx 1$. This implies that in region II, the micelle size is mainly determined by the fraction of loop chains. Note that the micelles in this system are formed through the assembly of A blocks. Since each loop chain contributes two A blocks to the micelle, while a bridge chain contributes only one A block, it is reasonable that higher f_{loop}

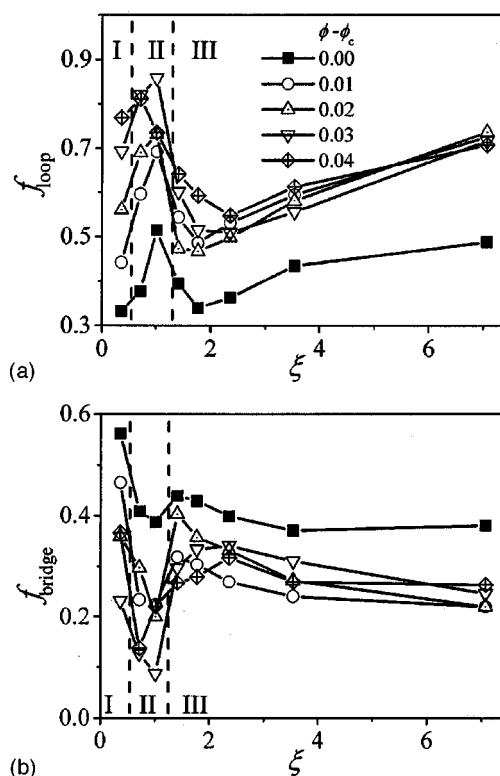


FIG. 4. The conformation distribution vs the size ratio and the volume fraction at the sol-gel transition regime: (a) the loop conformation fraction plot with the size ratio and (b) the bridge conformation fraction as a function of the size ratio.

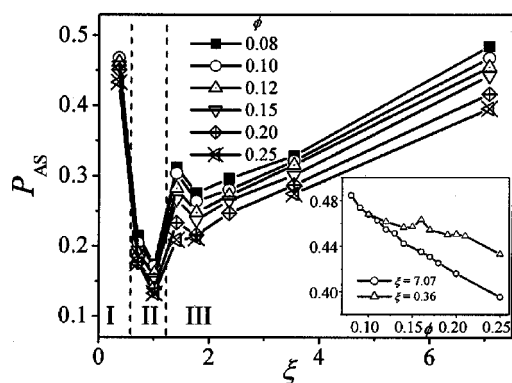


FIG. 5. The reduced interaction pair P_{AS} vs the size ratio at different volume fractions. The inset is the dependence of P_{AS} on the volume fraction at two different size ratios.

will lead to bigger micelle size. In region II, f_{loop} is much higher than that in regions I and III, which may be due to the extra potential induced by the solvent greatly affecting the conformation distribution on the microscale.

Until now, we do not know much about the coexistence state between the solvent and the polymer chains, i.e., whether the polymer chains are swollen by the solvent or they are separate. To explore this issue, we introduce the reduced effective interaction pair between the monomers in A blocks and solvent segments, which is defined as

$$P_{AS} = \langle N_{AS} \rangle / zn_p l_p, \quad (4)$$

where N_{AS} is the total interaction pairs in each sample, z is the effective coordination number, which equals 14 in this model,⁵⁰ and the $\langle \rangle$ denotes the ensemble average of 25 samples at each size ratio and volume fraction. From Fig. 5, it can be seen that with increasing volume fraction, P_{AS} decreases remarkably in region III, and in regions I and II, the decrease is much smaller (the inset), i.e., in regions I and II, the interactions between the components of the system become insensitive to the volume fraction, implying that the system is more like a bulk. With decreasing size ratio, P_{AS} first decreases and reaches a minimum in region II before quickly bouncing back to the value close to that for a normal solvent. The P_{AS} values in region II are very small, indicating that the polymer chains and the middle-sized solvent molecules tend to separate rather than dissolve. The data of the interaction pairs between the B blocks and solvent segments exhibit a similar trend (data not shown). Therefore, we conclude that phase separation between the polymer and the solvent has occurred in region II.

Based on the above results, we correlate the effect of the solvent size with the physical gelation mechanism in triblock copolymer solutions as follows.

In region I, the size of the solvent molecule is so large that the system can be considered as a miscible polymer blend. The polymer is in a bulklike state, and gelation occurs at high polymer concentrations. The micelles are small, and the micelle size distribution becomes narrower with increasing volume fraction of the polymer. Thus the gelation is dominated by the crowd and the arrest of the micelle and the polymer chains, which must be similar to a glasslike kinetic arrest process and follow the glass transition mechanism.^{17–22}

In region II, the solvent size approaches the ideal end-to-end distance of the polymer chain, i.e., the solvent is the so-called middle-sized solvent. The gelation occurs at very low polymer concentrations. The micelles are large, and the micelle size distribution broadens with increasing volume fraction of the polymer, and the gelation takes place with the concomitant of phase separation. Therefore, the gelation mechanism is a phase separation and random aggregation one.^{23–27}

In region III, the solvent size is normal or quasinormal, and the polymer chains are swollen. The gelation occurs at high polymer concentrations. The micelles are small, and the micelle size distribution either slightly decreases or shows no clear trend with increasing volume fraction, and the gelation is dominated by the population of the chains with bridge conformation or loop conformation.^{28–33}

SUMMARY

In this work, we investigated triblock copolymer solutions with solvents of various sizes. From macroscale to microscale, the sol-gel coexistence phase diagram, the aggregation behavior and the conformation distribution of the polymer influenced by the solvent size have been analyzed in detail. Phase separation has also been observed when the length of the solvent molecules approaches the ideal end-to-end distance of the polymer chains. Particularly, we found that physical gelation follows three different mechanisms when the solvent size is much larger than the ideal end-to-end distance of the polymer chain, or is in the middle-sized solvent region, or is in the normal or quasinormal solvent region, respectively.

ACKNOWLEDGMENTS

This work is supported by the National Natural Science Foundation of China (NSFC) for the General Program (Grant Nos. 20304015 and 50373044), the Key Program (Grant No. 20334010), the Major Program (Grant Nos. 20490220 and 50390090), the National Science Fund for Distinguished Young Investigators (Grant No. 59825113), and the Chinese Academy of Sciences (Grant No. KJCX2-SW-H07) and subsidized by the Special Funds for Major State Basic Research Projects (Grant No. 2003CB615600).

¹W. A. Pekta, J. L. Harden, K. P. McGrath, D. Wirtz, and D. A. Tirrell, *Science* **281**, 389 (1998).

²F. C. MacKintosh, J. Käs, and P. A. Janmey, *Phys. Rev. Lett.* **75**, 4425 (1995).

³B. Hinner, M. Tempel, E. Sackmann, K. Kroy, and E. Frey, *Phys. Rev. Lett.* **81**, 2614 (1998).

⁴J. Kopecek, *Nature (London)* **417**, 388 (2002).

⁵J. H. Laurer, J. F. Mulling, S. A. Khan, R. J. Spontak, and R. Bukovnik, *J. Polym. Sci., Part B: Polym. Phys.* **36**, 2379 (1998).

⁶Z. Hu, Y. Chen, C. Wang, Y. Zheng, and Y. Li, *Nature (London)* **393**, 149 (1998).

⁷R. J. P. Corriu and D. Leclercq, *Angew. Chem., Int. Ed.* **35**, 1420 (2003).

⁸M. Ilavský, H. Inomata, A. Khokhlov *et al.*, *Adv. Polym. Sci.* **109**, 1 (1993).

⁹J. H. Burban, E. L. Cussler, S. H. Gehrke *et al.*, *Adv. Polym. Sci.* **110**, 1 (1993).

¹⁰M. J. Song, D. S. Lee, J. H. Ahn, D. J. Kim, and S. C. Kimi, *Polym. Bull. (Berlin)* **43**, 497 (2000).

¹¹Y. Zhao, Y. Cao, Y. Yang, and C. Wu, *Macromolecules* **36**, 855 (2003).

- ¹²M. P. S. R. Nágila, B. H. Sara, Y. Zhuo, C. Valeria, W. H. Ian, Y. Xue-Feng, A. David, and B. Colin, *Langmuir* **20**, 4272 (2004).
- ¹³T. A. Walker, J. J. Semler, D. N. Leonard, G. J. van Maanen, R. R. Bukovnik, and R. J. Spontak, *Langmuir* **18**, 8266 (2002).
- ¹⁴J. M. Yu, Ph. Dubois, P. Teyssié, R. Jérôme, S. Blacher, F. Brouers, and G. L'Homme, *Macromolecules* **29**, 5384 (1996).
- ¹⁵K. Kuroda, K. Fujimoto, J. Sunamoto, and K. Akiyoshi, *Langmuir* **18**, 3780 (2002).
- ¹⁶S. K. Kumar and J. F. Douglas, *Phys. Rev. Lett.* **87**, 188301 (2001).
- ¹⁷J. Bergenholz and M. Fuchs, *Phys. Rev. E* **59**, 5706 (1999).
- ¹⁸V. Trappe, V. Prasad, L. Cipelletti, P. N. Segre, and D. A. Wei, *Nature (London)* **411**, 772 (2001).
- ¹⁹P. N. Segrè, V. Prasad, A. B. Schofield, and D. A. Weitz, *Phys. Rev. Lett.* **86**, 6042 (2001).
- ²⁰A. M. Puertas, M. Fuchs, and M. E. Cates, *Phys. Rev. E* **67**, 031406 (2003).
- ²¹S. R. Bhatia and A. Mourchid, *Langmuir* **18**, 6469 (2002).
- ²²F. Mallamace, P. Gambadauro, N. Micali, P. Tartaglia, C. Liao, and S. H. Chen, *Phys. Rev. Lett.* **84**, 5431 (2000).
- ²³K. Kobayashi, C. Huang, and T. P. Lodge, *Macromolecules* **32**, 7070 (1999).
- ²⁴M. Hirrien, C. Chevillard, J. Desbrières, M. A. V. Axelos, and M. Rinaudo, *Polymer* **39**, 6251 (1998).
- ²⁵J. R. Quintana, E. Diaz, and I. Katime, *Macromol. Chem. Phys.* **197**, 3017 (1996).
- ²⁶M. J. Park and K. Char, *Langmuir* **20**, 2456 (2004).
- ²⁷J. Borgström, M. Egermayer, T. Sparrman, P. O. Quist, and L. Piculell, *Langmuir* **14**, 4935 (1998).
- ²⁸A. Kelarakis, V. Havredaki, X. F. Yuan, Y. W. Yang, and C. Booth, *J. Mater. Chem.* **13**, 2779 (2003).
- ²⁹D. A. Vega, J. M. Sebastian, Y. L. Loo, and R. A. Register, *J. Polym. Sci., Part B: Polym. Phys.* **32**, 2183 (2001).
- ³⁰F. Tanaka, *Macromolecules* **33**, 4249 (2000).
- ³¹F. Tanaka and T. Koga, *Comput. Theor. Polym. Sci.* **10**, 259 (2000).
- ³²F. Tanaka and T. Koga, *Bull. Chem. Soc. Jpn.* **74**, 201 (2001).
- ³³Y. Q. Li, Z. Y. Sun, T. F. Shi, and L. J. An, *J. Chem. Phys.* **121**, 1133 (2004).
- ³⁴M. Fuchs and K. Schweizer, *J. Phys.: Condens. Matter* **14**, R239 (2002).
- ³⁵K. N. Pham, A. M. Puertas, J. Bergenholz *et al.*, *Science* **296**, 104 (2002).
- ³⁶X. Ye, T. Narayanan, P. Tong, and J. S. Huang, *Phys. Rev. Lett.* **76**, 4640 (1996).
- ³⁷R. Tuinier, J. Rieger, and C. G. de Kruif, *Adv. Colloid Interface Sci.* **103**, 1 (2003).
- ³⁸D. Zhou, L. Li, Y. Li, J. Zhang, and G. Xue, *Macromolecules* **36**, 4609 (2003).
- ³⁹D. Zhou, L. Li, B. Che, Q. Cao, Y. Lu, and G. Xue, *Macromolecules* **37**, 4744 (2004).
- ⁴⁰N. B. Wilding, M. Müller, and K. Binder, *J. Chem. Phys.* **105**, 802 (1996).
- ⁴¹I. Carmesin and K. Kremer, *Macromolecules* **21**, 2819 (1988).
- ⁴²H. P. Deutsch and K. Binder, *J. Chem. Phys.* **94**, 2294 (1991).
- ⁴³K. Binder and D. W. Heermann, *Monte Carlo Simulation in Statistical Physics* (Springer, Berlin, 1992).
- ⁴⁴J. Lu and Y. Yang, *Sci. China, Ser. A: Math., Phys., Astron. Technol. Sci.* **11**, 1229 (1991).
- ⁴⁵N. Metropolis, A. W. Rosenbluth, M. N. Rosenbluth, and A. H. Teller, *J. Chem. Phys.* **21**, 1087 (1953).
- ⁴⁶P. G. de Gennes, *Scaling Concepts in Polymer Physics* (Cornell University Press, Ithaca, NY, 1979).
- ⁴⁷D. Stauffer and A. Aharony, *Introduction to Percolation Theory* (Taylor & Francis, London, 1992).
- ⁴⁸M. Nguyen-Misra and W. L. Mattice, *Macromolecules* **28**, 1444 (1995).
- ⁴⁹Y. Bohbot-Raviv, T. M. Snyder, and Z.-G. Wang, *Langmuir* **20**, 7860 (2004).
- ⁵⁰H. P. Deutsch and K. Binder, *J. Chem. Phys.* **94**, 2294 (1991).